Nonlinear parametric resonances in quasiperiodic dispersion oscillating fibers

Christophe Finot, Alexej Sysoliatin, Stefan Wabnitz

Nonlinear parametric resonances in aperiodic dispersion oscillating fibers

Christophe Finot [1,*] , Alexej Sysoliatin [2], and Stefan Wabnitz [3]

[1] *Laboratoire Interdisciplinaire Carnot de Bourgogne, UMR 5209 CNRS-Université de Bourgogne, 9 avenue Alain Savary, BP 47870, 21078 Dijon Cedex, France*

[2] *Fiber Optics Research Center, 11933 Moscow, Russia*

[3] *Dipartimento di Ingegneria dell'Informazione, Università degli Studi di Brescia, and Istituto Nazionale d'Ottica, CNR, via Branze 38, 25123, Brescia, Italy*

[*] *Corresponding author:*
E-mail address: christophe.finot@u-bourgogne.fr
Tel.: +33 3 80395926

Abstract: We numerically study the evolution of the spectrum of parametric resonance or modulation instability sidebands in aperiodic dispersion oscillating fibers. We separately consider a linear variation along the fiber of either the spatial period, the average dispersion, or the amplitude of the dispersion oscillation. We found that this linear variation of the dispersion oscillating fiber parameters may provide different novel mechanisms for the splitting of the resonance sideband spectrum, owing to coherent interference between quasi-resonant waves that are generated at different points along the fiber.

Keywords: Dispersion oscillating fiber, modulation instability, four-wave mixing

1. Introduction

Modulation instability (MI) is a nonlinear process that has been widely investigated in various fields of physics including plasmas, hydrodynamics and optics, to cite a few. In the presence of a high power continuous wave (CW), MI leads to the emergence and amplification of gain sidebands in the wave spectrum. In nonlinear fiber optics, such a process has been demonstrated in fibers with anomalous, constant group velocity dispersion (GVD) [1], as well as in normal GVD fibers by enabling the fulfillment of the nonlinear phase-matching condition through either fourth order dispersion [2; 3], birefringence or a multimodal structure [4; 5; 6]. However, the efficiency of such parametric processes may highly suffer from unwanted longitudinal fluctuations of the fiber parameters, with a rapid drop of the gain as well as a broadening of its bandwidth. Ultimately, parametric gain may fully disappear in the presence of fiber fluctuations [4; 5; 6], which leads to the requirement of sophisticated devices or fiber designs [2; 3; 6; 7; 8]. The efficiency of pulse reshaping processes may also be seriously impaired by stochastic fluctuations of the fiber parameters [9].

To the contrary, whenever the longitudinal variations of the fiber parameters are quite large, periodic and controlled such as in loss (or nonlinearity) [10], dispersion [11] or polarization [12; 13] managed fiber transmission or laser systems, new deterministic MI or parametric resonance (PR) sidebands appear. In this work, we shall use the terms of MI or PR as fully equivalent in our description of the sideband spectrum generation process. As a matter of fact, the periodic oscillation of the fiber dispersion leads to the quasi-phase-matching (QPM) of the nonlinear four-wave mixing (FWM) process. As a result, unequally spaced MI sidebands can emerge [14]. A renewed experimental and theoretical interest in these studies has been recently stimulated by the availability of fibers presenting a longitudinal and periodic modulation of their dispersion

properties [12; 15]. Recent experimental works have confirmed the QPM-induced MI process in the normal GVD regime of microstructured dispersion oscillating fiber (DOF) around 1 μm [16; 17], as well as of non-microstructured highly nonlinear DOF at telecom wavelengths [16].

However, one may wonder how in this case deviations from a strictly periodic evolution of the fiber parameters may affect the QPM-MI spectrum. Can it be beneficial to the enlargement of the sideband bandwidth to use a chirped DOF, in a manner that is similar to the approach commonly used in the context of chirped QPM quadratic crystals? Or is the longitudinal variation of the parameters of the fiber always detrimental to the parametric resonance gain? To answer this important question, in this work we numerically study the impact of a linear longitudinal evolution of the main parameters of a DOF. Therefore our analysis is organized as follows. In a first section, we describe our numerical model and the specific DOF under investigation. Next, by using systematic simulations and an approximate approach that is based on the Floquet theorem and the associated linear stability analysis, we separately discuss the influence of each parameter, i.e., the spatial dispersion oscillation period, the value of the average dispersion, and finally the amplitude of the dispersion oscillations.

2. Model and situation under investigation

The evolution of the optical field ψ in an optical fiber can be described by the nonlinear Schrödinger equation (NLSE) that includes both the Kerr nonlinearity γ and the longitudinally varying second-order dispersion $\beta_2(z)$

$$i\frac{\partial\psi}{\partial z}-\frac{\beta_2(z)}{2}\frac{\partial^2\psi}{\partial t^2}+\gamma|\psi|^2\psi=0 \qquad (1)$$

where ψ is the complex electrical field, z is the propagation distance and t is the reduced time.

MI or parametric resonance induced by the longitudinal variations of chromatic dispersion was theoretically investigated before in a wide range of configurations, ranging from sinusoidal profiles with a spatial period of a few tens of meters [18; 19], up to dispersion-managed systems with periods of several kilometers [16; 18]. Let us consider a fiber dispersion profile that evolves with distance *z* according to the following sinusoidal rule

$$b_2(z) = b_{2av} + b_{2amp}\sin\left(2pz/\mathrm{L}\right), \tag{2}$$

where Λ is the spatial period of the dispersion oscillation, β_{2av} is the average dispersion of the fiber, and β_{2amp} is half of the peak-to-peak amplitude of the dispersion variation. In the presence of sinusoidal longitudinal GVD variations, and when pumped by a continuous wave of power *P*, the QPM of FWM (or MI, or PR) leads to the appearance of resonant gain sidebands, whose angular frequency shift relative to the pump can be analytically predicted as follows [12; 13; 20; 21] :

$$\Omega_p^2 = \frac{2\pi p/\Lambda - 2\gamma P}{\beta_{2av}} \tag{3}$$

with $p = 1, 2, 3\ldots$ The corresponding exponential gain coefficient for the p^{th} sideband may be estimated by the analytical expression [12] :

$$g\left(\Omega_p\right) = 2\gamma P\left|J_p\left(\frac{\beta_{2amp}\,\Omega_p^2}{2\pi/\Lambda}\right)\right| \tag{4}$$

where J_p is the Bessel function of order *p*.

In this contribution, we analyze by means of extensive numerical simulations the spectrum of parametric resonances in a quasi-periodic DOF. Specifically, we consider a linear variation with

propagation distance z of each of the three parameters in the right hand side of Eq.(2). By expressing any of these parameters as Q, we set

$$Q(z) = \bar{Q}\left(\alpha\frac{z}{L}+1-\frac{\alpha}{2}\right) \tag{5}$$

Here Q stands for either Λ, β_{2av}, or β_{2amp}; $\bar{Q}$ is the average value of the quantity under study, and α characterizes the rate of evolution of Q. Positive values of α indicate that the value of the Q parameter grows larger along the propagation distance. The ratio of the peak-to-peak amplitude of fluctuation ΔQ over $\bar{Q}$ is $|\alpha|$. The values of the parameters Q_0 and Q_L at the input and output of the fiber are therefore $Q_0 = \bar{Q}\left(1-\frac{\alpha}{2}\right)$ and $Q_L = \bar{Q}\left(1+\frac{\alpha}{2}\right)$, respectively.

Inspired by the highly nonlinear DOF that was experimentally used in [22], we consider here a DOF with the following average values: $\bar{\Lambda}$ =20 m, $\overline{\beta_{2av}}$ = 2 ps^2.km^{-1} and $\overline{\beta_{2amp}}$ = 2 ps^2.km^{-1}. We set the overall fiber length equal to 400 m, and its nonlinear coefficient γ = 10 W^{-1}.km^{-1}. The DOF is pumped by a CW pump with the average power P = 4 W at the telecommunication wavelength λ=1550 nm. Examples of the resulting dispersion profiles for the different cases of linear variation of either one of the Λ, β_{2av}, or β_{2amp} parameters are illustrated in Fig. 1.

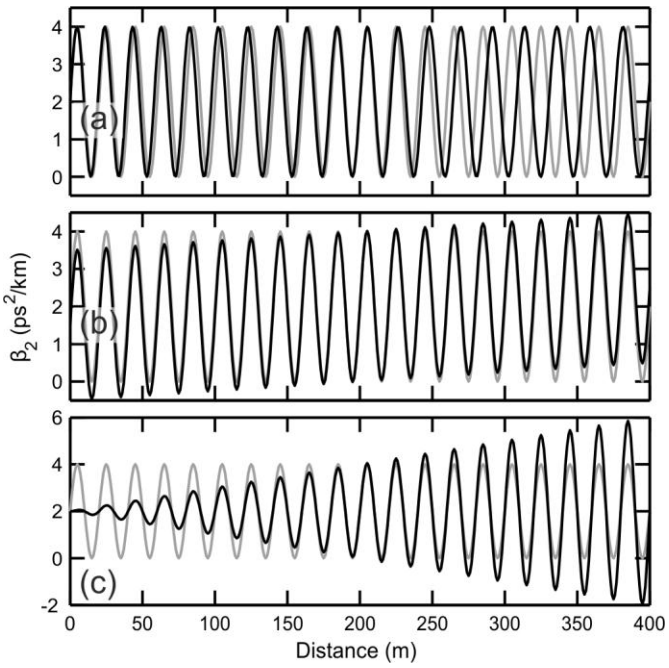

Figure 1 : Evolution of the longitudinal dispersion profile of a DOF with sinusoidal dispersion modulation (grey line), or for a quasi-periodic DOF with linear evolution of either: the spatial period (panel a, black line, $\alpha = 0.1$); the average dispersion (panel b, black line, $\alpha = 0.5$); the amplitude of the dispersion fluctuations (panel c, black line, $\alpha = 2$).

We numerically solved the NLSE (1) by the standard split-step Fourier algorithm, including a weak input white noise seed: the results were averaged over 12 independent noise shots. We consider here separately the impact of a longitudinal variation of either Λ, β_{2av}, or β_{2amp}. We also took advantage of the LSA based on the Floquet theorem, which proved to be a very powerful tool for the analysis of the evolution of the MI gain spectrum in DOFs [18; 19; 23]. Clearly the Floquet theorem is strictly valid for a periodic DOF only: nevertheless, it may still be used as an approximate tool to compute the sideband spectrum in quasi-periodic DOFs as well. Indeed, in Ref. [17; 21; 24; 25] we have shown that the Floquet method may still be used to obtain an approximate averaged description of the MI gain spectrum in the presence of fiber loss (or gain). The way to compute the gain profile $g(\omega, Q)$ by the Floquet method is to consider first a constant

value of Q, obtain its corresponding PR spectrum, and then compute the overall MI spectrum g_F by simply averaging over the probability distribution of the Q parameter

$$g_F(\omega) = \int g(\omega, Q)\ pdf(Q)\ dQ = \int_{Q_0}^{Q_L} g(\omega, Q)\ \ dQ \tag{6}$$

3. Impact of the spatial period variation

We start our study by investigating the influence of a spatial dispersion oscillation period that varies linearly with the propagation distance (see Fig. 1(a)). The resulting spectra (or Arnold resonance tongues [24]) are plotted in Fig. 2(a), and highlight the rapid fall of the gain that is experienced by the various sidebands when $|\alpha|$ is increased. We may also note that the unequally spaced and initially narrow spectral sidebands continuously broaden and eventually may overlap. The splitting and fan-out of the resonant sideband frequencies is strikingly reminiscent to the Stark splitting of the electron resonances or spectral lines of atoms and molecules in the presence of an applied electric field [26; 27]. Moreover, Fig. 2(a) also shows that an oscillatory pattern develops in the sideband amplitudes within the resonance tongues. In Fig. 2(b), we evaluate the tolerance $\Delta\alpha_p$ on α, that we defined as follows: $\Delta\alpha_p = \alpha_{\max} - \alpha_{\min}$ where $\alpha_{\max}$ and $\alpha_{\min}$ are the values of α leading to a decrease of 10 dB of the maximum gain of the p^{th} sideband. $\Delta\alpha_p$ rapidly decreases with the order of the gain sideband, from a value of 0.26 for the first sideband down to a value below 0.05 for the 6$^{\text{th}}$ sideband. As a practical consequence, we may infer that even very small deviations from a strictly periodic dispersion oscillation structure may hamper the development of high-order gain sidebands, and that a tight drawing precision is therefore required for generating a large set of spectral lines.

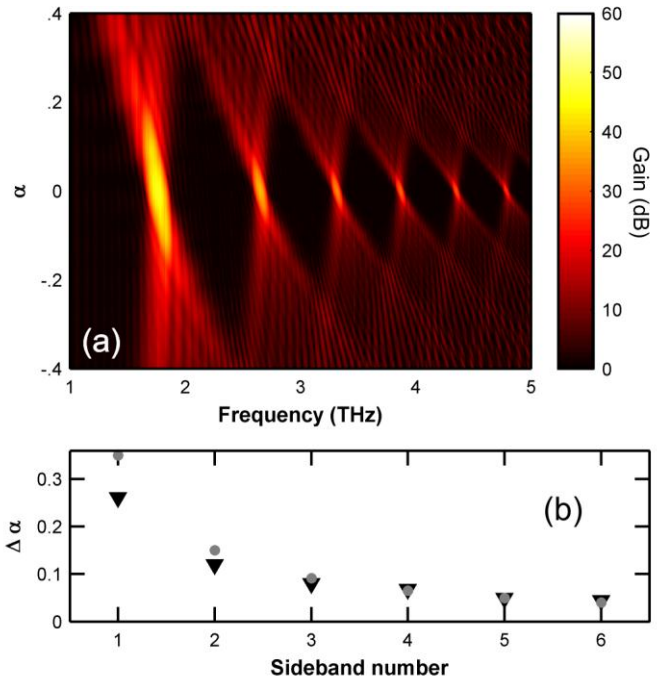

Figure 2 : (a) Evolution of the MI gain spectrum (or Arnold resonance tongues) according to the amplitude of the linear change of the spatial period. Results are obtained from the numerical integration of the NLSE. **(b)** Evolution of $\Delta\alpha$ at -10dB according to the QPM sideband number *p*: results from numerical simulations (black triangles) are compared with results from the Floquet LSA (grey circles)

Details of the spectra obtained for α = -0.1 and α = 0.1 are provided in Fig. 3(a1), and compared with the gain spectrum that obtained in perfectly periodic conditions. We may note here that the sign of α has a crucial influence on the sideband spectrum, as can also be observed by noting the tilt of the spectrum in Fig. 2(a). In other words, according to the direction of propagation along the chirped DOF, the sideband spectrum may exhibit a shift towards either lower or higher frequencies whenever the dispersion oscillation period grows larger or smaller, respectively.

In order to gain a simple qualitative understanding of the observed evolution of the resonance tongues, we computed the corresponding sideband spectrum as it is predicted by the Floquet

linear stability analysis: Fig. 3(b) summarizes the evolution of the gain $g(\omega,\Lambda)$ for a strictly periodic DOF. In agreement with the analytical expression for the sideband position given in Eq. (3), the central frequencies of the gain sidebands are strongly affected by changes of the oscillation period Λ. This explains the observed broadening of the average gain profile resulting from Eq. (6) (see Fig. 3(c)), as well as the dramatic decrease of the gain values. Quite unexpectedly, the approximate Floquet method approach may indeed qualitatively well reproduce the numerically observed gain drop that is summarized in Fig. 2(b). Nevertheless, the Floquet method approach is unable to capture some of the numerically observed features, such as the previously discussed spectral asymmetry of the sideband spectrum obtained as the direction of propagation is reversed in the linearly chirped DOF. Clearly, the main a limitation inherent in using Eq. (6) is that the average gain is a sum of positive contributions: the overall gain may intrinsically only increase upon propagation. Hence it is not possible to reproduce with Eq. (6) the large spectral oscillations of the gain sidebands: as it can be seen in Fig. 3(a2), instead of strong oscillations, a kind of plateau is predicted. This means that the sideband splitting and associated rapid amplitude oscillations with frequency of the resonance tongues are due to the coherent constructive (or destructive) interference among the sidebands that are generated at different points along the chirped DOF. Moreover, Eq. (6) leads to the same result irrespective of the sign of α: consequently, it fails in predicting the asymmetric spectral evolution that is obtained by the full numerical simulation of the NLSE.

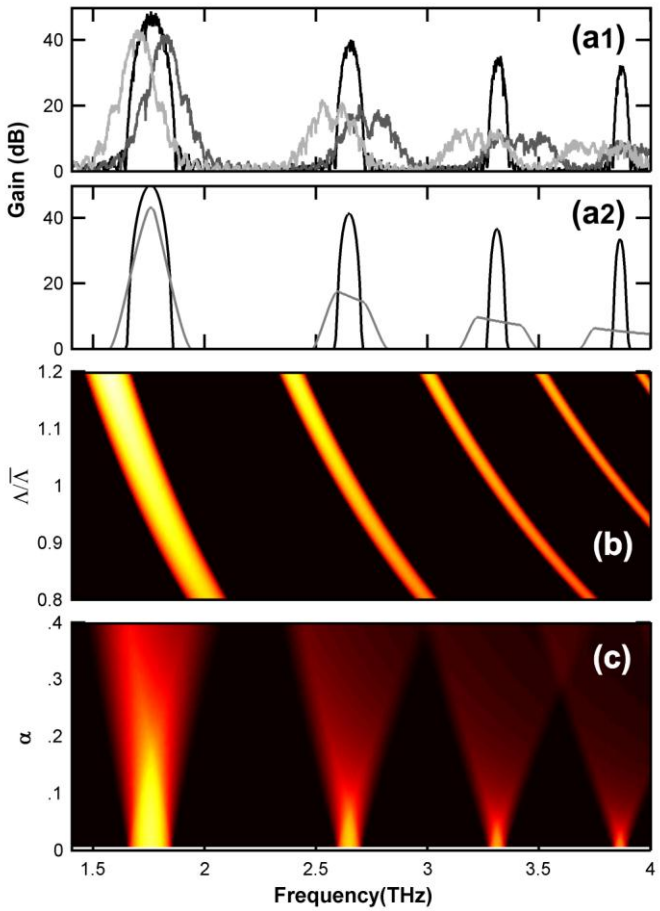

Figure 3 : (a) Output spectrum obtained from numerical simulations (panel a1) without linear evolution of Λ (black line), for α = -0.1 (grey curve) and α = 0.1 (light grey curve). Result from Eq. (6) are plotted on panel (a2) for $|\alpha|$ = 0.1 (grey line). **(b)** Evolution of the QPM MI spectrum $g(\omega)$ according to Λ for a strictly periodic DOF, as predicted by the Floquet LSA. **(c)** Evolution of the output spectrum according to $|\alpha|$ as predicted by the use of the approximate approach based on Eq. (6). Same colormap as Fig. 2.

4. Impact of the average dispersion variation

Let us investigate next the influence on the Arnold resonance tongues of a longitudinal change of the average DOF dispersion (see Fig. 1(b)). To this end, we carried out a numerical study similar to that of section 3. The corresponding results are summarized in Fig. 4 and Fig. 5. As it can be seen in Fig.4, in this case the sideband splitting and fan-out as the amplitude of the average dispersion excursion grows larger is now symmetric with respect to the direction of variation of α (or β_{2av}). On the other hand, we may also note from Figs.4-5 several features that are common with the trends observed in the presence of a chirped spatial period Λ. Namely, the broadening to the gain sidebands results owing to the change of Ω_p according to β_{2av} as predicted by Eq.(3). Moreover, the peak sideband gain is strongly sensitive to the presence of a chirp: its amplitude drops and exhibits strong frequency oscillations. Finally, an overlap of the different gain sidebands is also observed in Fig.4 and Fig.5. Once again, in spite of some limitations owing to the fact that the Floquet method is only rigorously applicable to a perfectly periodic DOF, the approximate approach that is based on Eq. (6) may provide a useful insight on the evolution of the gain bandwidth or the range of $\Delta\alpha$. But even if the difference between DOF with constant parameters and the aperiodic DOF under study seem relatively small (see Fig. 1(b) plotted for α= 0.5), Eq. (6) is unable to capture the rapidly oscillating spectral pattern that is observed when the gain sideband spectrum is substantially broadened. Once again, the sideband splitting and amplitude oscillations within the Arnold resonance tongues result from the coherent (or phase-sensitive) summation of sidebands generated at different points of the linearly chirped DOF.

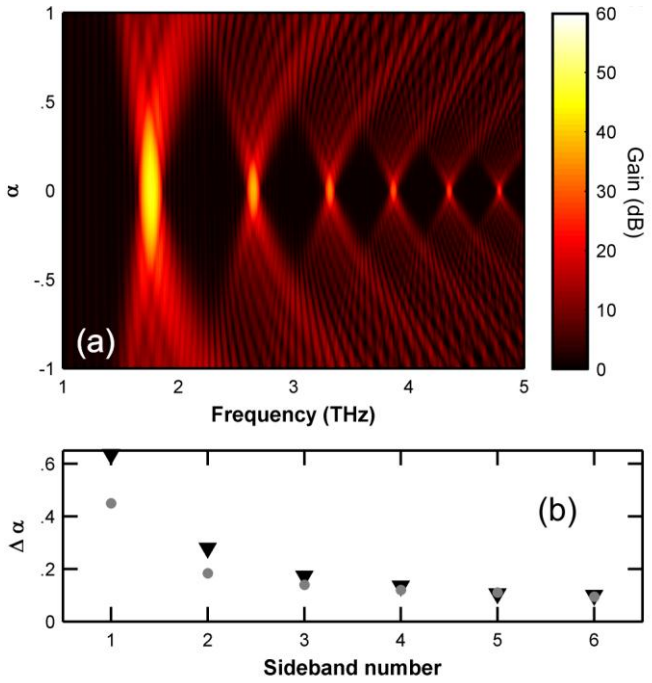

Figure 4 : (a) Evolution of the MI gain spectrum or resonance tongues vs. the amplitude of the linear variation of the average dispersion. Results are obtained from the numerical integration of the NLSE. **(b)** Evolution of $\Delta\alpha$ at -10dB vs. the QPM sideband order: results from numerical simulations (black triangles) are compared with results from the Floquet LSA (grey circles)

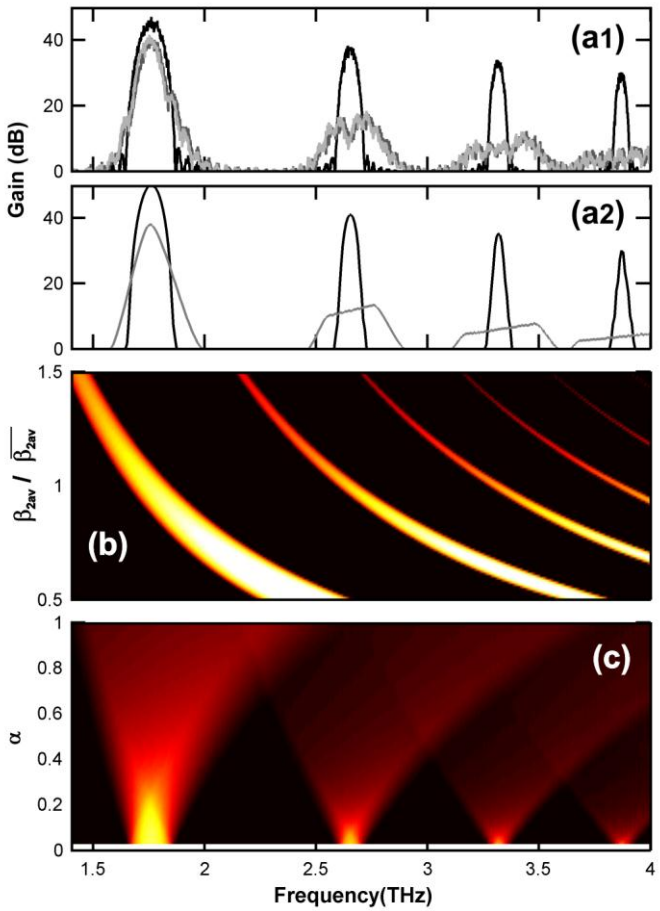

Figure 5 : (a) Output spectrum obtained from numerical simulations (panel a1) without a linear evolution of β_{2av} (black curve), and for α = -0.25 (grey line) or α = 0.25 (light grey curve). Result from Eq. (6) are plotted on panel (a2) for $|\alpha|$ = 0.25 (grey curve). **(b)** Evolution of the QPM MI spectrum according to β_{2av} for a strictly periodic DOF as predicted by the Floquet linear stability analysis. **(c)** Evolution of the output spectrum according to $|\alpha|$ as predicted by the use of the approximate approach based on Eq. (6). Same colormap as Fig. 4.

5. Impact of the amplitude of the dispersion oscillation

In this last section, we shall examine the impact of a linear variation of the amplitude of the fiber dispersion oscillation on the shape and amplitude of the Arnold resonance tongues. As we shall see, in this case the evolution of the sideband spectrum is strongly dependent on the value of the (constant) average dispersion β_{2ave}. Let us consider first the case with β_{2ave} = 2 ps^2/km. The corresponding results, obtained from the numerical integration of the NLSE, are summarized on Fig. 6(a). As it can be seen, in this case the linear chirp of the oscillation amplitude has a quite limited impact on the sideband spectrum, contrary to the two previous cases discussed in sections 2 and 3. Remarkably, Fig.6(a) shows that α may vary over a relatively large range, without significantly affecting the peak gain values. Indeed, Fig. 6(b) confirms that $\Delta\alpha$ may be as high as 3 and even higher, without decreasing the gain in the first QPM by more than 3 dBs. We may also note that the gain bandwidth does not broaden significantly, even when deviations from constant β_{2amp} as large as $\alpha = 2$ are imposed (see Fig. 1(c) for an illustration of the dispersion evolution for $\alpha = 2$). Finally, Fig. 6(a) shows that the spectrum deformation is fully symmetric as the sign of α is changed. This means that in this case the same spectrum results at the output of the chirped DOF, irrespective of the propagation direction.

Now, a relatively good qualitative and quantitative match is obtained between the numerical spectra and the approximate analysis relying on the Floquet LSA as it has been summarized in Fig. 7. The key point is that, contrary to the previous cases, the variation of the amplitude of the dispersion oscillations β_{2amp} should in principle have no influence, on the basis of Eq. (3), on the position of the MI sidebands.

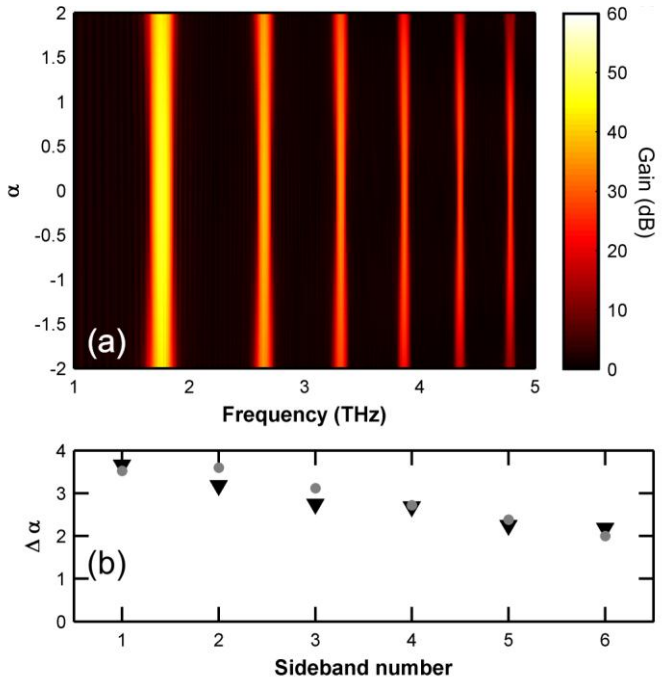

Figure 6 : (a) Evolution of the MI gain spectrum or resonance tongues vs. the strength of the variation of the dispersion oscillation amplitude; here β_{2av} = 2 ps^2/km. Results are obtained from the numerical integration of the NLSE. **(b)** Evolution of $\Delta\alpha$ at -3dB according to the order of the QPM sideband: results from numerical simulations (black triangles) are compared with approximate results from the Floquet LSA (grey circles).

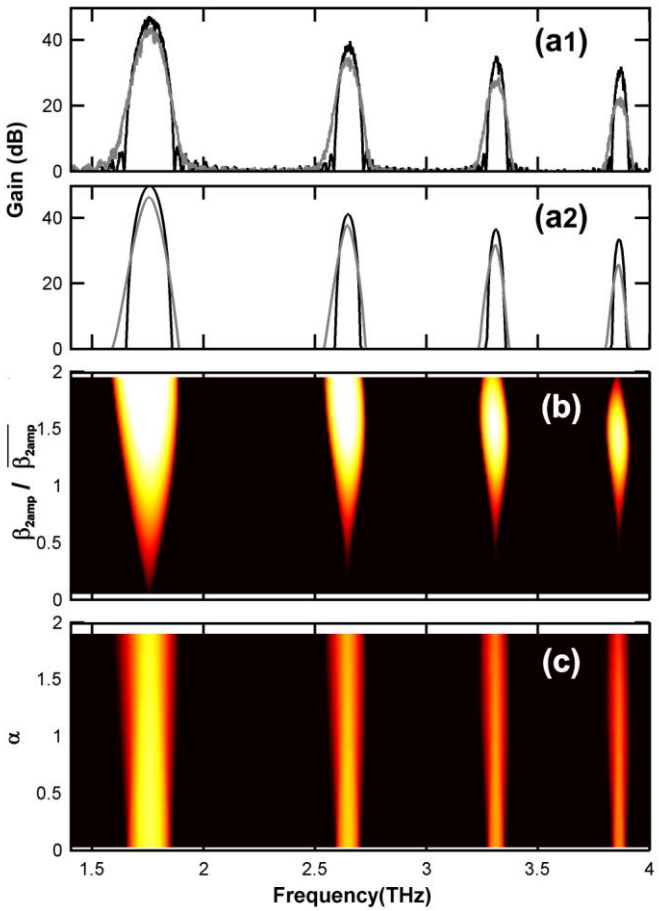

Figure 7 : (a) Output spectrum obtained from numerical simulations (panel a1) and from Eq. 6 (panel a2) for a constant β_{2amp} (black curve), and for α = 2 (grey curve); here β_{2av} = 2 ps^2/km. **(b)** Evolution of the QPM MI spectrum according to β_{2amp} for a strictly periodic DOF as predicted by the Floquet LSA. **(c)** Evolution of the output spectrum according to $|\alpha|$ as predicted by the use of the approximate approach based on Eq. (6). Same colormap as Fig. 6.

As we shall see now, the impact of the longitudinal evolution of β_{2amp} is dramatically different whenever the average dispersion is reduced down to β_{2ave}=1ps^2/km. The corresponding results of our systematic simulations are reported in Fig. 8(a): as can be seen, the resonance tongues display several new features. First of all, at low $|\alpha|$ values, a new sideband that is induced by FWM between the pump and the first QPM sideband is observed. The corresponding generation efficiency drops down as soon as the gain of the first QPM sideband decreases.

However, an interesting and novel property of the MI or PR spectrum is that for selected sidebands, the linearly chirped oscillation amplitude leads to a substantial increase of the spectral gain. This is for example the case for the 4th sideband: the corresponding gain is increased by more than 20 dBs with respect to the case of a strictly periodic DOF (see Fig. 8(c)). This gain enhancement may be explained with the help of Eq. (4): with $\alpha = 0$ and for the parameters under study, the gain predicted by Eq. (4) for the 4th sideband vanishes. To the contrary, whenever $\alpha \neq 0$, nonzero gain is experienced at different stages of the propagation along the fiber, so that the overall gain is finite. The numerically observed gain enhancement of Fig. 8(c) is well reproduced with the help of Eq. (6): the corresponding LSA results are presented in Fig. 9(b).

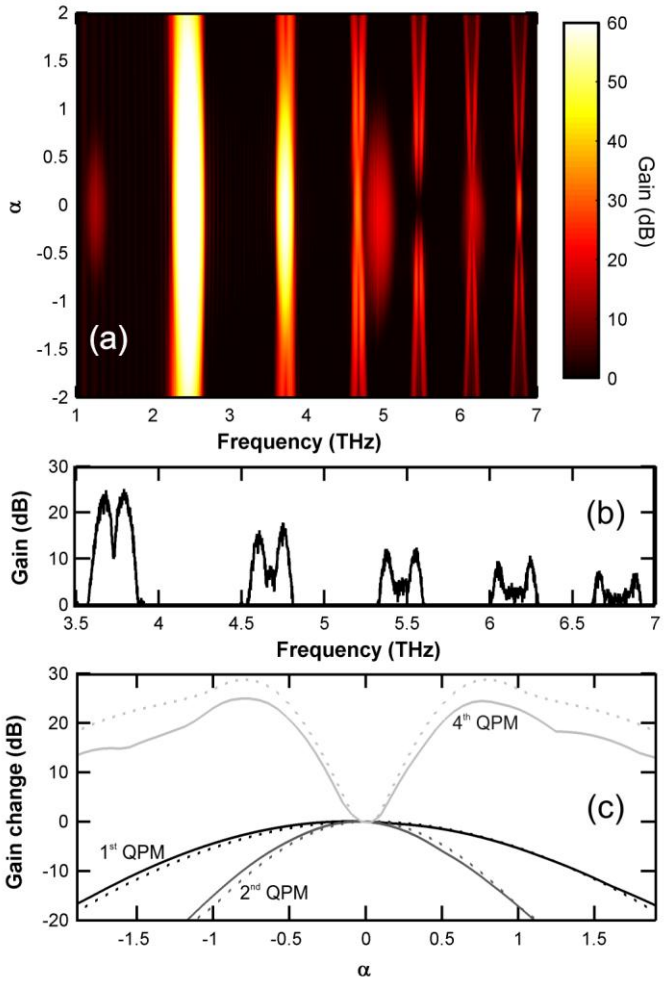

Figure 8 : (a) Evolution of the MI gain spectrum as a function of the value of the linear amplitude change of the dispersion fluctuations: here β_{2av} = 1 ps^2/km. Results are obtained from the numerical integration of the NLSE. **(b)** Details of the output spectrum recorded for α=2. **(c)** Evolution of the maximum value of the sideband gain vs. α for various sidebands (black, dark grey and light grey are for the first, second and fourth QPM sideband, respectively). Results from the numerical integration of the NLSE (solid curves) are compared with predictions from Eq. (6) (dotted curve).

On the other hand, in a manner similar to the cases described in Fig. 2 and Fig.4, the use of the Floquet approach based on the incoherent summation of Eq.(6) is not able to capture a very interesting spectral feature that is observed for the higher-order QPM sidebands in Figs. 8(b) and 9(a). As can be seen, instead of a spectral sideband with a single peak, a splitting into two separate sub-peaks occurs for sidebands of order p>1. Moreover, for each of these sidebands the frequency spacing between the two sub-peaks grows larger as $|\alpha|$ increases. The observed sideband splitting is analogous to the Zeeman splitting of the spectral lines in a gas in the presence of a strong magnetic field owing to the two states of the spin of the electron [28].

A sideband splitting of the resonance tongues was previously theoretically reported for a strictly periodic DOF in Ref. [29], and later experimentally demonstrated in Ref. [24], and its potential implications for all-optical signal processing were further analyzed in Ref. [23]. Because of the periodicity of the dispersion oscillations, in those cases the Floquet analysis could be successfully applied to reproduce the sideband splitting effect. In the case of a linearly chirped DOF, a proper extension of the Floquet method should be developed, similarly to the case of quasi-periodic (i.e., containing several incommensurable frequencies) parametric forcing [30]. However the development of this new mathematical tool is beyond the scope of the present numerical study. . In [31], Mussot et al analyzed analytically and experimentally the emergence of new sidebands in the spectrum obtained after propagation in a fiber with a complex dispersion oscillating profile characterized by two different spatial frequencies. We do not see here straightforward connections to the splitting highlighted in the fiber we investigate so that additional elements may be involved in the emergence of those peaks located at the edges of the gain sidebands.

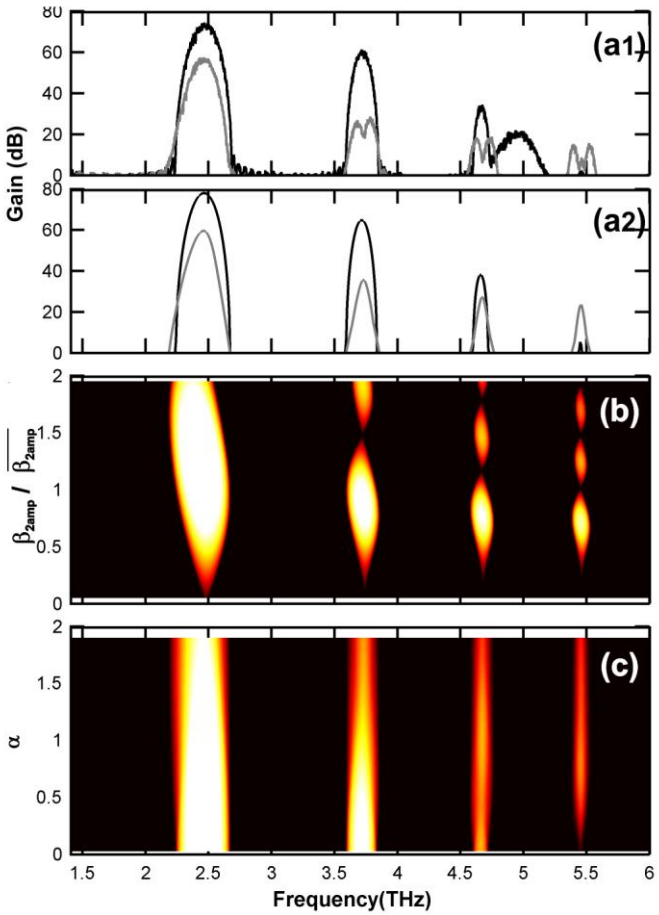

Figure 9 : Same as Fig. 7 but for β_{2av} = 1 ps^2/km. Same colormap as Fig. 8.

In the present case, the sideband splitting results from a coherent interference among the resonant waves that are generated at different points of the chirped DOF. The longitudinal evolution of the sideband amplitudes is illustrated on Fig. 10(a): as can be seen, the MI or PR gain at the mid-point of higher-order (i.e., with p>1) sidebands may experience a non-monotonic behavior. The initial growth is followed by a gain decrease at the mid-point of each parametric resonance. Correspondingly, two gain peaks emerge with a frequency spacing that grows progressively larger with the propagation distance.

We thus performed a systematic study of the evolution of the resonance tongues as a function of the value of the average dispersion. The corresponding results are summarized on Fig. 10(b), and reveal that the spacing between the sub-sidebands also increases with the ratio β_{2amp}/β_{2av}, so that two well-separated peaks may result, as the relative amplitude of the dispersion oscillations grows larger. Fig.10(b) reveals that the sideband splitting is not necessarily restricted to higher order QPM sidebands: for average dispersion β_{2av} <0.5 ps^2/km, a splitting of the first-order QPM sideband may be observed, too.

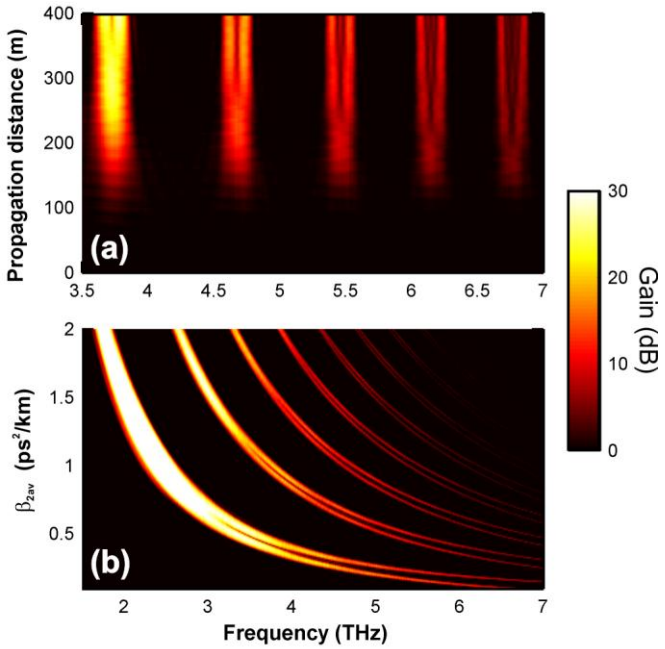

Figure 10 : (a) Longitudinal evolution of the QPM MI gain spectrum in a fiber with $\alpha = 2$ and $\beta_{2av} = 1$ ps^2/km. **(b)** Output spectrum according to the value of β_{2av} for $\alpha = 2$.

6. Conclusion

In this work we have studied how a longitudinal and linear evolution of the parameters of a dispersion oscillating fiber may affect the spectrum of quasi-phase-matched modulation instability or parametric resonance. We found that even slight deviations of a constant spatial period significantly affect the output sideband spectrum, in a manner that is sensitive to the direction of use of the DOF. Moreover, variations of the average DOF dispersion also impact the MI gain, leading to a noticeable sideband broadening, and the development of additional amplitude modulations in the sideband gain. To the contrary, as long as the ratio of sideband amplitude fluctuations to average dispersion β_{2amp}/β_{2av} remains moderately high, even large changes of the amplitude of the dispersion fluctuations do not significantly affect the main properties of the spectrum. On the other hand, in the regime of sufficiently high β_{2amp}/β_{2av} ratios, a new type of spectral sideband splitting was observed. In all of the above cases, a simple but approximate approach based on the averaging of Floquet spectra obtained by a linear stability analysis was found to be useful, and it could permit to qualitatively reproduce most of the observed spectral sideband features. However, the sideband splitting effect could not be captured by the averaged Floquet approach, since it results from a coherent constructive or destructive interference among the resonant waves generated at different points along the linearly chirped DOF.

Acknowledgements

We thank Julien Fatome and Kamal Hammani for stimulating discussions. We acknowledge the financial support of the Conseil Regional de Bourgogne (Pari Photcom), the funding of the Labex ACTION program (ANR-11-LABX-01-01), and the Italian Ministry of University and Research (grant no. 2012BFNWZ2).

References

[1] K. Tai, A. Hasegawa, and A. Tomita, Observation of modulational instability in optical fibers. Phys. Rev. Lett. 56 (1986) 135-138.

[2] G.K.L. Wong, A.Y.H. Chen, S.G. Murdoch, R. Leonhardt, J.D. Harvey, N.Y. Joly, J.C. Knight, W.J. Wadsworth, and P.S.J. Russell, Continuous-wave tunable optical parametric generation in a photonic-crystal fiber. J. Opt. Soc. Amer. B 22 (2005) 2505-2511.

[3] S. Pitois, and G. Millot, Experimental observation of a new modulational instability spectral window induced by fourth-order dispersion in a normally dispersive single-mode optical fiber. Opt. Commun. 226 (2003) 415-422.

[4] S. Wabnitz, Modulational polarization instability of light in a nonlinear birefringent dispersive medium. Phys. Rev. A 38 (1988) 2018.

[5] J.E. Rothenberg, Modulational instability for normal dispersion. Phys. Rev. A 42 (1990) 682.

[6] B. Kibler, C. Billet, J.M. Dudley, R.S. Windeler, and G. Millot, Effects of structural irregularities on modulational instability phase matching in photonic crystal fibers. Opt. Lett. 29 (2004) 1903-1905.

[7] M. Karlsson, Four-wave mixing in fibers with randomly varying zero-dispersion wavelength. J. Opt. Soc. Am. B 15 (1998) 2269-2275.

[8] M. Farahmand, and C.M. De Sterke, Parametric amplification ini presence of dispersion fluctuations. Opt. Express 12 (2004) 136-142.

[9] B.P.P. Kuo, J.M. Fini, L. Grüner-Nielsen, and S. Radic, Dispersion-stabilized highly-nonlinear fiber for wideband parametric mixer synthesis. Opt. Express 20 (2012) 18611-18619.

[10] B. Kibler, and C. Finot, Impact of structural irregularities on high bit rate pulse compression techniques in photonic crystal fibre. Electron. Lett. 44 (2008) 1011-1013.

[11] F. Matera, A. Mecozzi, M. Romagnoli, and M. Settembre, Sideband instability induced by periodic power variation in long-distance fiber links. Opt. Lett. 18 (1993) 1499-1501.

[12] N.J. Smith, and N.J. Doran, Modulational instabilities in fibers with periodic dispersion management. Opt. Lett. 21 (1996) 570.

[13] S. Ambomo, C.M. Ngabireng, P.T. Dinda, A. Labruyère, K. Porsezian, and B. Kalithasan, Critical behavior with dramatic enhancement of modulational instability gain in fiber

systems with periodic variation dispersion. Journal of the Optical Society of America B 25 (2008) 425-433.

[14] S.G. Murdoch, R. Leonhardt, J.D. Harvey, and T.A.B. Kennedy, Quasi-phase matching in an optical fiber with periodic birefringence. J. Opt. Soc. Am. B 14 (1997) 1816-1822.

[15] F.K. Abdullaev, S.A. Darmanyan, A. Kobyakov, and F. Lederer, Modulational instability in optical fibers with variable dispersion. Phys. Lett. A 220 (1996) 213-218.

[16] M. Droques, A. Kudlinski, G. Bouwmans, G. Martinelli, and A. Mussot, Experimental demonstration of modulation instability in an optical fiber with a periodic dispersion landscape. Opt. Lett. 37 (2012) 4832-4834.

[17] A. Armaroli, and F. Biancalana, Tunable modulational instability sidebands via parametric resonance in periodically tapered optical fibers. Opt. Express 20 (2012) 25096-25110.

[18] C. Finot, J. Fatome, A. Sysoliatin, A. Kosolapov, and S. Wabnitz, Competing four-wave mixing processes in dispersion oscillating telecom fiber. Opt. Lett. 38 (2013) 5361-5364.

[19] F. Feng, J. Fatome, A. Sysoliatin, Y.K. Chembo, S. Wabnitz, and C. Finot, Wavelength conversion and temporal compression of a pulse train using a dispersion oscillating fibre. Electron. Lett. 50 (2014) 168-170.

[20] F. Consolandi, C. De Angelis, A.-D. Capobianco, G. Nalesso, and A. Tonello, Parametric gain in fiber systems with periodic dispersion management. Opt. Commun. 208 (2002) 309-320.

[21] J.C. Bronski, and J.N. Kutz, Modulational stability of plane waves in nonreturn-to-zero communications systems with dispersion management. Opt. Lett. 21 (1996) 937-939.

[22] M. Droques, A. Kudlinski, G. Bouwmans, G. Martinelli, and A. Mussot, Dynamics of the modulation instability spectrum in optical fibers with oscillating dispersion. Phys. Rev. A 87 (2013) 013813.

[23] F. Feng, P. Morin, Y.K. Chembo, A. Sysoliatin, S. Wabnitz, and C. Finot, Experimental demonstration of gain sideband splitting in dispersion oscillating fibers. Opt. Lett. in press (2015) preprint available on https://hal.archives-ouvertes.fr/hal-01092503.

[24] C. Finot, F. Feng, Y.K. Chembo, and S. Wabnitz, Gain sideband splitting in dispersion oscillating fibers. Opt. Fiber. Technol. 20 (2014) 513-519.

[25] A. Armaroli, and F. Biancalana, Suppression and splitting of modulational instability sidebands in periodically tapered optical fibers because of fourth-order dispersion. Opt. Lett. 39 (2014) 4804-4807.

[26] H. Broer, J. Puig, and C. Simó, Resonance tongues and instability pockets in the quasi–periodic Hill–Schrödinger equation. Commun. Math. Phys 241 (2003) 467-503.

[27] H. Broer, and C. Simó, Resonance tongues in Hill's equations: a geometric approach. Journ. Diff. Eqns 166 (2000) 290-327.

[28] J. Stark, Beobachtungen über den Effekt des elektrischen Feldes auf Spektrallinien. I. Quereffekt (Observations of the effect of the electric field on spectral lines I. Transverse effect). Annalen der Physik 43 (1914) 965-982.

[29] P. Zeeman, Doublets and triplets in the spectrum produced by external magnetic forces. Phil. Mag. 44 (1897) 55-60.

[30] C. Finot, and S. Wabnitz, On the influence of the pump shape on the modulation instability process induced in a dispersion oscillating fiber. (2015) preprint available at https://hal.archives-ouvertes.fr/hal-01103031.

[31] J.A. Murdock, On the Floquet problem for quasiperiodic systems. Proc. Of the American Mathematical Society 68 (1978) 179-184.